The Hypersonic Experiment SHEFEX – Aerothermodynamic Layout, Vehicle Development and First Flight Results

Thino Eggers[(1)], Andreas Stamminger[(2)], Marcus Hörschgen[(3)], Wolfgang Jung[(3)], John Turner[(4)]

[(1)]Deutsches Zentrum für Luft- und Raumfahrt (DLR), Institute of Aerodynamics and FLow Technology, Lilienthalplatz 7, 38108 Braunschweig, Tel.: +49-531-295-2436, Fax: +49-531-295-2320, Email: thino.eggers@dlr.de
[(2)]Deutsches Zentrum für Luft- und Raumfahrt (DLR), RB-MR, D-82234 Wessling, Tel.: +49-8153-28-2616, Fax:+49-8153-28-1344, Email: andreas.stamminger@dlr.de
[(3)]Deutsches Zentrum für Luft- und Raumfahrt (DLR), RB-MR, D-82234 Wessling, Tel.: +49-8153-28-2606
[(4)]TwIG, contracted by Deutsches Zentrum für Luft- und Raumfahrt (DLR), RB-MR D-82234 Wessling

Abstract – The purpose of the SHarp Edge Flight Experiment SHEFEX was the investigation of the aerodynamic behaviour and thermal problems of possible new shapes for future launcher or re-entry vehicles. The main focus was the improvement of common space vehicle shapes by application of facetted surfaces and sharp edges. The experiment has permitted the accurate investigation of the flow effects and their structural solution during the hypersonic flight from 90 km down to an altitude of 20 km. The project, performed under responsibility of the German Aerospace Centre (DLR) was launched from Andoya Rocket Range, Norway on October 27th 2005. This paper introduces the mission, describes the layout of the experiment and the re-entry vehicle, as well as the development process of the complete flight vehicle and initial post flight results.

1 – Introduction

The objective of the SHEFEX experiment was the investigation of a facetted Thermal Protection System (TPS) concept and the assessment of the potential of sharp edged configurations applying the three point strategy: numerics - ground based facilities - flight experiment. The motivation is neither to perform a re-entry experiment nor to fly at the thermal boundary of modern high temperature materials but to prove with flight evidence that the temperature peaks at the edges of the ceramic-composite panels are lower than those predicted based on a radiation equilibrium hypothesis.

From the aerodynamic point of view, the design of a hypersonic vehicle is affected by finding a compromise between a vehicle being sharp enough to obtain acceptable aerodynamic and propulsion efficiency and blunt enough to reduce the aerodynamic heating. Therefore, during the 1990s, the development of ceramic composite and ultra high temperature materials for TPS applications led to a renewed interest in sharp edged configurations such as the waverider concept DLR F8 [1], the DLR-ONERA project JAPHAR [2] or the lifting body concept HL-20 and the SHARP project, both from NASA [3], [4]. The current experiment SHEFEX is presented here.

Driven by the facetted concept, two main criteria have been used to define the aerodynamic shape of SHEFEX. It should have as many as possible facetted panels and it should represent as many as possible configuration details of space vehicles, like concave and convex chamfers and a sharp unswept leading edge. The experiment should enable a detailed investigation of the flow effects and their structural solution during flight.

At first sight, the technical requirements for the performance of the SHEFEX mission appeared relatively straight forward. The achievement of hypersonic velocities up to Mach 7 between the altitudes of 90 to 20 km on the descent required a ballistic trajectory with an apogee of less than 300 km. The anticipated payload mass of the order of only 200-250 kg and the budget limitations, suggested the use of a two stage motor combination comprising a military surplus Improved Orion as second stage and a Brazilian S30 motor as first stage, a vehicle which had already been successfully launched. It was obvious that the payload alone would not be stable on re-entry and so it was decided to leave the burnt out second stage with fins, attached to the payload. A further obvious requirement was to realign the vehicle with the velocity vector during the exo-atmospheric descent to minimise aerodynamic drag induced deceleration and perturbed flight and point the experiment with close to zero angle of attack during the re-entry and experiment phase. The only aspect which seemed to pose obvious problems from the beginning was the recovery of the experiment and the

major part of the instrumentation which, considering a completion of the experiment phase at 20 km altitude and with a vertical velocity in excess of 2000 m/sec, does not leave a lot of time to separate the payload from the motor and perform a parachute deployment recovery sequence. In the three year duration of this project, the team was faced with an abundance of unusual problems and has now successfully launched one of the most interesting and demanding sounding rockets which we have ever constructed.

2 – The Experiment

The experiment is shown in **Fig. 1** and described in detail in [5] to [7]. It consisted of an asymmetric facetted form of 830 mm length and about 350 mm at the base, comprising multiple flat panels with sharp edges. An aluminium support structure housed a large number of pressure, temperature and heat flux sensors and to this structure were attached the flat panels made of ultra high temperature ceramics which, together with flexible ceramic felt insulation, provided the TPS. The use of flat panels reduces the cost of tooling, manufacture and inspection of the TPS and the sharp edges provide improved aerodynamic performance over blunt nosed vehicles at hypersonic velocities. The asymmetric form was designed to provide a correlation of the theoretical estimates and wind tunnel measurements of the thermal loads and aerodynamic lift of such forms at hypersonic velocities. The facetted experiment form was connected to the payload cylinder by an adapter which provided a relatively smooth aerodynamic transition to the payload cylinder.

3 – The SHEFEX Mission

The SHEFEX launcher was a two-stage solid propellant sounding rocket system conceived primarily for ballistic microgravity experiments. The first stage was a Brazilian S 30 motor and the second stage an improved ORION (**Fig. 2**). Between the facetted forebody and the second stage were two cylindrical modules which housed the recovery system, the main electronics, the data acquisition devices, the power supply and the cold gas thruster system for the Attitude Control System (ACS) (**Fig. 3**). During the ascent the facetted forebody was protected by an ogive nose cone.

The projected mission is schematically sketched in (**Fig. 4**). It is a suborbital flight mission launched from Andoya (Norway). The first stage burns out after 28 sec and separates from the rest of the launcher at an altitude of 17 km. The second stage burns out after 56 sec at an altitude of 65 km. Since the facetted body has no control devices the second stage remains attached to the payload with facetted body until the end of the experiment, to provide flight stability with its fins (Fig. 3). At about 90 km, the nose cone separates and a cold gas ACS initiates the pointing maneuver. The apogee is reached at approx. 300 km. No yo-yo de-spinning maneuver is necessary since the ACS eliminates any remaining spin. The planned SHEFEX experiment startes on the descent at an altitude of 90 km and continues with a mean Mach number of up to 7 down to an altitude of 20 km. Thus, a measurement time of approx. 45 sec is available for measurements on hypersonic flow effects. The selected flight path fits rather well inside the operational range of the high enthalpy ground facilities of DLR, allowing numerical and ground based data correlations with flight measurements.

4 – Aerothermodynamic Layout of the Reentry Vehicle

The aerodynamic and aerothermodynamic studies were performed based on calculations with the DLR Euler- and Navier-Stokes Code TAU [8] applying unstructured grids. The main purpose of the aerothermodynamic analysis of the SHEFEX forebody was the assessment of the expected heatloads and a first analysis of the flow field. At the beginning an average flight Mach number of M=7.5 was assumed. Hence, the results represent the upper limit of the expected thermal loads. The calculations cover the complete Reynolds number range of $70.000 < Re < 3.500.000$. Dependent on the altitude the boundary layer is assumed to be fully laminar or fully turbulent. The wall was assumed to behave radiation adiabatic (ε=0.83). The analysis of the surface values of pressure, temperature and heat flux are the basis for the choice of the flight instrumentation and the positioning of the sensors. **Fig. 5** and **Fig. 6** illustrate the influence of the boundary layer state on the flow field and the surface temperature. Although the forebody is very simple, a complex and interesting flow field is obtained. In the backward part of the lower surface which is intended to simulate conditions of a deflected control surface parallel to the hinge line a separation is obtained which

clearly decreases in case of a turbulent boundary layer. Additionally, the coloured streamlines show, that along the highly swept corner of the second forebody-segment a small vortex is obtained (see enlarged view of Fig. 5). This vortex hits on the backward inclined panel and induces a local hotspot as shown in Fig. 6. To capture this phenomenon the number of sensors are increased in these regions (Fig. 1). Altogether, the experiment has 40 thermocouples, 5 heat flux sensors, 8 pressure sensors, 1 pyrometer and 3 accelerometers. The surface temperatures indicate that except of the unswept leading edge of the forebody never a critical temperature with view to the resilience of the ceramic panels is reached. The shown temperatures are a measure for the upper temperature limit because they represent the never obtained steady state conditions without taking into account the structural heat conductivity.

One critical point of the configuration is the step appearing between forebody and the first cylindrical segment (**Fig. 7**). Here, heat loads in the order of those at the unswept leading edge are expected. In any case structural failures due to thermal loads or shock-shock interactions have to be prevented because they would end in the destruction of the vehicle. Therefore, special emphasis is taken in the analysis of this region. By comparison of the lines of constant Mach number and the pressure coefficients the slip line which might be critical with view to the heat loads can be detected. The analysis of this region was mainly performed based on 2D calculations of the symmetry plane. The validity of this assumption is given by the comparison of a 3D and a 2D surface temperature distribution along the lower surface of the forebody (**Fig. 8**). Fig. 8 also shows that the separated hot boundary layer flow is redirected back into the separation bubble. This results in very high radiation adiabatic temperatures but it has to be taken into account that these results are steady state solutions and that the structural conductivity is neglected. If the high temperature area between slip line and shock is considered, it is obvious that thermal loads coming from this region will not affect the surface flow for the flow conditions expected to appear during the SHEFEX experiment. Additionally, one single Navier-Stokes calculation of the complete reentry vehicle was carried out in order to exclude severe problems corresponding to hot spots resulting from shock-shock / shock-boundary layer interactions. **Fig. 9** gives an idea about the flowfield between the lower side of the horizontal fin and the lower vertical fin. Due to shock / shock interactions, a high temperature region is obtained in the corner between the lower side of the horizontal fin and tail can. Although the obtained temperatures are in the order of 1500K this region is not considered to be critical because the temperatures are smaller than those of the fin leading edges. Additionally, these temperatures represent a worst case scenario, because the fully heated state will not be reached due to the short flight time.

5 – Requirements for the Aerodynamic Layout

Driving design factors for both, the re-entry experiment vehicle and the launch vehicle, were the experiment's requirements. These included a controlled and stable descent flight without any spin-up and at best, zero angle of attack (AoA), especially in the axis containing the experiment asymmetry. To meet these requirements, considerable modifications to the original concept for the re-entry vehicle have been essential, always keeping in mind that the slightest changes from the standard flight proven configuration, significantly affect the ascent behaviour, particularly the vehicle's stability and performance. Investigations had to consider the complete vehicle system from launch to impact and work out a compromise between experiment goals and technical feasibility.

6 – Aerodynamic Layout of the Re-entry Vehicle

Initial aerodynamic investigations including computational fluid dynamics (CFD) analysis of the re-entry stability, indicated a major problem in the pitch axis which is the axis containing the experiment asymmetry. During descent into denser layers of the atmosphere, the experiment body induces lifting forces which considerably exceed the control capability of the standard three fin combination on the motor or the torque of the attitude control system and leads to an uncontrollable increase in AoA. An extensive aerodynamic study was performed to find an optimum position for both, the centre of pressure (CoP) and the centre of gravity (CoG). First steps to increase stability were modifications in motor and payload cylindrical length by adding spacer modules. The number of fins on the second stage was increased to four and their area slightly enlarged. This strategy was severely limited by the fact that more and bigger fins on a second stage, shifts the CoP of the two stage vehicle forward and decreases the static stability margin during first stage burn and in any case the resulting CoP improvement was marginal.

Stabilizing flap mechanisms and movable fins were briefly considered but then discarded due to complexity. Approaches to move the CoG more forward by rearranging the payload modules and installing ballast mass were ineffective as the heavy burnt out second stage motor case does not permit a significant CoG shift. **Fig. 10** shows pitch instability for various re-entry configurations for a flight velocity of Mach 7.5. The corresponding neutral point position (x_N) is displayed above the vehicles, the CoG was fixed with 47% from nose tip. The positive slope of the pitching moment curve indicates an instable flight mode. The end result of all of these calculations with respect to the minor modifications was that re-entry stability could only be achieved with a drastic CoG shift of up to 8% which was not realizable. It was apparent that a deeper layout investigation and redesign was necessary.

A study on the stabilizing effects of flared sections on rockets led to the exchange of the standard boat tail by a conical flare on the Improved Orion. Several different flare cone lengths and angles were considered showing an optimum at the standard tail can length with an opening half angle of β=12 deg. Finally, with adapted and enlarged fins on the flare, stable re-entry behaviour in pitch could be realised even when degrading the CoG position slightly with the increased mass of the flare at the aft end. Based on this new layout, the complete interstage section had to be modified as well. The standard Nike to Improved Orion interstage adapter was attached to a newly designed S30 motor adapter and fairing, providing a smooth stage transition and low mass.

7 – Aerodynamic Layout of the Launch Vehicle

Continuing with ascent stability calculations, the design changes on the second stage caused the expected problems regarding static margin and performance. As a solution, the standard fins for the S30 motor were exchanged for the newly developed second stage fin set from the VSB-30 vehicle. Unfortunately, the VSB-30 tail can assembly with three fins still showed a lack of stability and this heavy load bearing version increased lift-off mass considerably. Again a modification to this tail can was carried out by replacing the former integral construction by a light weight ring and sheet tail can supporting four VSB-30 second stage fins. Now sufficient stability also for the up-leg was assured (**Fig. 11**). As a positive side effect of the interstage redesign it turned out to noticeably reduce drag in the supersonic speed region and hereby compensate the clearly higher vehicle total mass. With this layout, trajectory calculations resulted in an apogee of approximately 270 km guaranteeing the desired re-entry velocities, displayed in **Fig. 12**.

8 – Vehicle Improvement and Consensus

Now with a generally feasible vehicle configuration, the improvement phase on detail level started with investigations on the resulting descent AoA in pitch and associated loads on the vehicle, stability in yaw and roll, stage separation and thermal loads. **Fig. 13** shows the scaled comparison of the standard vehicle configuration with the newly designed experimental vehicle. A final trim to an AoA of close to zero degrees would have required such a large amount of ballast mass as to reduce the vehicle performance to an unacceptable level.

As a compromise, a resulting maximum AoA of approximately three degrees for trimmed flight is obtained by integrating a 20 kg experiment adapter in the payload forward section. **Fig. 14** presents the calculated AoA versus the pitching moment coefficient as a function of Mach number. The corresponding bending loads for this comparatively high AoA were taken as design criteria for component layout including a margin of one degree. Stability in yaw is not considered as critical because the vehicle is fully symmetrical in the yaw plane, with the large Orion fins counteracting any perturbations.

It is usual to offset (cant) the fins of all stages to provide spin stabilization during the ascent phase, however, to ensure a non spinning flight on the down-leg, the second stage fins have to have zero offset. As a result of flight parameter computation, the induced spin rate with first stage fin incidence of around 1.0 Hz will abruptly drop down to zero after stage separation (see Fig.11). This leads to higher impact dispersion and less stability during the further ascent, especially for second stage ignition, and complicates exact trajectory prediction. Even when increasing the first stage fin cant angle up to a maximum, the degrading effect in spin after separation remains. A possible reduction of the effects of this problem would be achieved by reducing the coast flight phase to four seconds, but this harbours some risk, as the tolerance in both first stage motor tail-off and the accuracy of the mechanical timers, which initiate the Orion ignition, could result in a pre separation ignition.

The modified interstage section also required investigations into the stage separation as simple aerodynamic drag separation is no more assured due to the flare and larger fins and consequent drag on the re-entry vehicle. To guarantee a safe separation before second stage ignition, a small gap between the motors is necessary, which is achieved by a spring driven separation unit, installed in the interstage section, pushing against the flared tail can and ensuring a separation at first stage burn-out.

Regarding the thermal loads on the vehicle components during the experiment phase, the choice in sophisticated material is limited and protection is realised by applying ablative coating on critical parts such as fin surfaces and particularly leading edges and flared tail can. The final flight vehicle system now represents the evolution of a standard sounding rocket adapted to the specific scientific requirements of hypersonic research vehicles which together with the SHEFEX experiment fore body constitute the complete experimental vehicle.

9 – Vehicle Subsystems and Component Development

Due to the stability problems that occurred during the aerodynamic layout several major modifications were necessary. The design of the Improved Orion (2^{nd} stage) tailcan and fins was driven by the requirements of a stable re-entry. For the fins a new design approach concerning ribs and frame was chosen which makes use of the evolution in manufacturing methods in the last decades. The stress that is induced in the fins by aerodynamic forces during ascent and especially during re-entry is distributed into the frame more efficiently. The SHEFEX flight showed that the fins have easily withstood bending forces and moments as presented in [9]. Due to the late separation in 14 km the dynamic pressure was higher than the layout conditions. The new tailcan design was based on the standard boattail version of the Improved Orion tailcan. For a FEM analysis a load of 5300 N on each fin and an additional 4000 N lift on the flared tailcan was assumed, which led to the stress distribution in **Fig. 15**. As already mentioned in the former section, the design changes on the second stage caused the expected problems regarding static margin and performance. As a solution, the standard fins for the S30 motor were exchanged for the newly developed second stage fin set from the VSB-30 vehicle. Unfortunately, the VSB-30 tail can assembly with three fins still showed a lack of stability and this heavy load bearing version increased lift-off mass considerably. Again a modification to this tail can was carried out by replacing the former integral construction by a light weight ring and sheet tail can supporting four VSB-30 second stage fins.

One of the main subsystems is the Attitude Control System (ACS). The main task of the ACS is to control the re-entry vehicle such that the experiment is aligned with close to zero angle of attack to the velocity vector during the descent into the atmosphere. During the ascent, the ACS must remove any residual spin after exiting the atmosphere and subsequent to ejection of nosecone, the vehicle pitch plane must be aligned with the trajectory plane. Prior to re-entry, the vehicle positive roll axis had to be aligned with the velocity vector.

The main sensor for the attitude control is a DMARS-R roll stabilised platform which contains a de-spun platform which isolates its two dynamically tuned gyros and three accelerometers from the usually high vehicle spin rate during the motor boost phase. The DMARS is an inertial grade sensor which provides not only attitude angles for the attitude control, but also accelerations, rates and position which were important for providing experimental data on the flight dynamics of the experiment. The DMARS internal computer which controls the platform and drift compensation and performs the navigation calculations and the coordinate transformations, is also used to perform the attitude control calculations and generate the thruster control signals [10].

The recovery operation consists of separation of the payload from the Orion motor at an altitude of approx. 15.6 km (50000 ft) on the descent and at a velocity of slightly more than 2000 m/sec. The separation system is a pyrotechnically actuated, high pressure gas manacle ring release and gas plunger system which is initiated by two redundant pressure switches attached to the recovery system pressure measurement manifold. The aerodynamic forces on the asymmetric experiment ensured that the payload quickly separated from the Orion motor and as it was inherently unstable, it tumbled and decelerated to an estimated velocity of the order of 250 m/sec. At an altitude of 3.5 km the recovery sequence should have been initiated by a barometric switch which ejects the heat shield and deployed a specially designed, high velocity drogue parachute. This 1.58 m² ribbon parachute was to be de-reefed after a 5 sec delay and decelerate the payload to 60 m/sec. After a further 10 sec, the 24.2 m² main tri-conical parachute should have been deployed in a reefed condition and then de-reefed after a further 5 sec, leading to a final sink velocity of 15 m/sec, before

sea impact. The main parachute contained a ram air filled 220 litre flotation bag for buoyancy attached to the canopy top and a recovery beacon.

10 – First Flight Results

SHEFEX was launched from the Andoya Rocket Range, Norway on 27th October 2005 at 13:45 UTC. Shortly after the flight it is not yet possible to present a detailed and profound investigation on the flight dynamics and behaviour of the complete and experimental vehicle. Nevertheless, some general facts of the vehicle performance as well as significant flight effects can be pointed out.

During flight the vehicle reached an apogee of 211 km which is 35 km lower than the expected altitude. See also **Fig. 16**. The difference in apogee from actual to the prediction is probably due to the lower than planned launcher elevation. For safety reasons the elevation of the launcher was set to 85° and the actual setting was below 83°. This led also to a higher ground range of 190 km. The actual azimuth was 325° but the final flight azimuth turned out to be 310°. The total flight time was 550 seconds comprising 45 seconds of experimental time for the atmospheric re-entry between 90 km and 14 km.

To avoid spin-up of the experimental vehicle during the re-entry phase only the first stage fins were canted inducing spin stabilization. At first stage burn-out after 28 seconds a roll frequency of 1.6 Hz could be detected including a slight coning motion, decreasing immediately as expected to zero at stage separation. But even without any design incidence on the second stage fins the vehicle started to build-up a roll in the opposite direction. On leaving the atmospheric influence region the spin rate was -0.8 Hz. A manual correction of this roll spin was necessary. At 80 seconds after lift-off the nosecone was ejected nominally.

The ACS roll control thrusters eliminated in the following 70 seconds all roll motion but consumed a significant amount of the gas reserve. After this, the pitch and yaw movements of the vehicle were controlled manually to set it to the calculated re-entry attitude. Due to lack of cold gas a slow tumble motion was remaining when the vehicle approached the atmosphere.

At little less than 120 km of altitude when first fin stabilization effects became obvious, the experimental vehicle started aligning itself to re-entry attitude. Pitch and yaw motions were reduced to an oscillation around the re-entry trim angle. When entering into thicker atmospheric layers the negative spin up effect observed during the second stage burn phase could be detected again resulting in vehicle roll of 1 Hz before payload separation and additional coning due to induced lift forces on the experiment forebody. The flight velocities during the atmospheric decent varied in the region of 1700 m/sec. The maximum velocity of 1870 m/s during re-entry was measured in an altitude of 27.8 km. The Mach number is relatively constant at a value of 5 from 100 km down to 50 km. Then the Mach number increases up to its maximum value 6.47 at 26 km. See also **Fig. 16**. From 100 km down to the payload separation it took only a time of around 50 seconds. When passing 25 km of altitude the onboard camera shows thermal degradation of the fin leading edges resulting in a sine shape deformation and glowing (see **Fig.17**). Temperature and pressure sensors provided data for the complete re-entry until an enormous increase of heat at payload separation. At 14 km of altitude the motor separation was initiated nominally by barometric switches. As predicted an enormous deceleration of the payload occurred during the following 3 seconds. This also resulted in an increase of recovery system manifold pressure up to 850 mbar. This impact pressure on the static pressure system caused the recovery sequence to be activated far too early, as it was also controlled by 15000 ft barometric switches (operating at 550 mbar). The flight velocity at this time was in the order of 1500 m/sec leading to an instantaneous loss of both parachute stages. The payload displayed stable flat spin motion on further decent decreasing velocity to 75-100 m/sec. As quick look data showed that the recovery system could not produce a soft landing and flotation in the water, the recovery vessel was recalled.

In summary it can be said from an initial analysis of the data received from the experiment and service systems that all major experiment aims were achieved proving that the novel TPS system worked according to the expectations. In the light of the enormous scientific data, the failure to recover the payload had only an insignificant effect on the success of the SHEFEX mission.

9 – References

[1] Strohmeyer, D.; Eggers, Th.; Haupt, M.: *Waverider Aerodynamics and Preliminary Design for Two-Stage-to-Orbit Missions*, Part 1, Journal of Spacecraft and Rockets, Vol. 35, No. 4, July-August 1998, pp. 450-458.

[2] Eggers, Th.; Novelli, Ph.; Haupt, M.: *Design Studies of the JAPHAR Experimental Vehicle for Dual Mode Ramjet Demonstration*, AIAA Paper 2001-1921, 2001.

[3] Reuther, J. et al.: *A Reusable Space Vehicle Design Study Exploring Sharp Leading Edges*, AIAA Paper 2001-2884, 2001.

[4] Arnold, J.; Johnson, S.; Wercinski, P.:SHARP: *NASA's Research and Development Activities in Ultra-High Temperature Ceramic Nose Caps and Leading Edges for Future Space Transportation Vehicles*, Proceedings of the 52nd International Astronautical Congress, IAF paper 01-V.5.02, France, October 2001.

[5] Longo, J.M.A.; Püttmann, N.: *The Sharp Edge Flight Experiment SHEFEX*, Proceedings of the DGLR Jahrestagung, DGLR-2004-072, September 2004

[6] Eggers Th. : *Aerodynamic and Aerothermodynamic Layout of the Hypersonic Flight Experiment SHEFEX*, 5th European Symposium on Aerothermodynamics for Space Vehicles, November 2004.

[7] Eggers Th., Longo J., Hörschgen M., Stamminger A. : *The Hypersonic Flight Experiment SHEFEX*, 13th AIAA/CIRA International Space Planes and Hypersonic System and Technologies Conference, May 2005.

[8] Mack, A.; Hannemann, V.: *Validation of the Unstructured DLR-TAU-Code for Hypersonic Flows*, AIAA Paper 2002-3111, 2002.

[9] Stamminger, A.; Turner, J.; Hörschgen, M.; Jung, W.: *Sounding Rockets as a Real Flight Platform for Aerothermodynamic CFD Validation of Hypersonic Experiments*, 5th European Symposium on Aerothermodynamics for Space Vehicles, Köln, Germany, November 2004.

[10] Turner, J.; Hörschgen, M.; Turner, P.; Ettl, J.; Jung, W.; Stamminger, A.: *SHEFEX – The Vehicle And Subsystems for a Hypersonic Re-Entry Flight Experiment*, 17th ESA Symposium on European Rocket and Balloon Programmes and Related Research, Sandefjord, Norway, June 2005.

10 – Figures

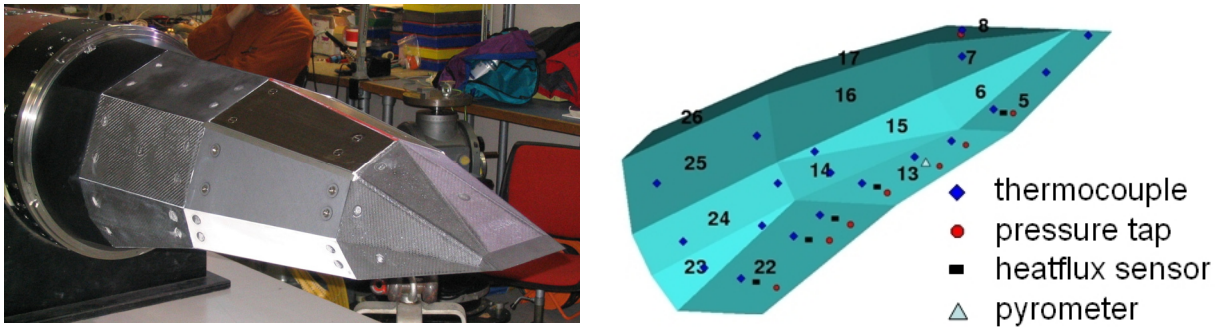

Fig. 1: SHEFEX Experiment

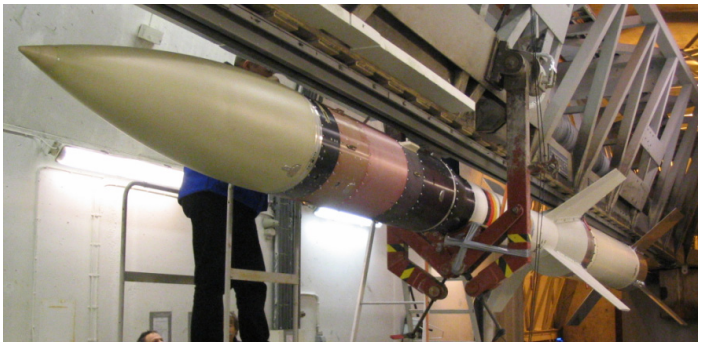

Fig. 2: SHEFEX launcher on launch pad

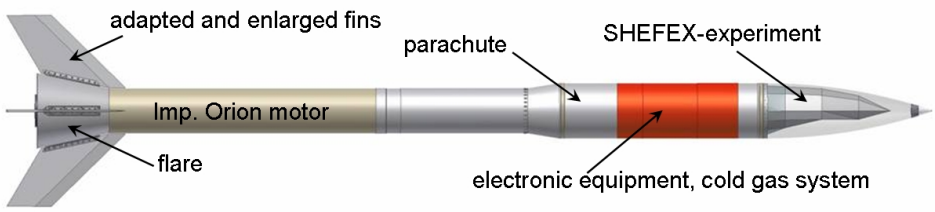

Fig. 3: SHEFEX reentry configuration

Time [sec]	Altitude [km]	Action
t_0	0	1st stage ignition and vehicle lift-off
t +28	17.5	1st stage burnout and stage separation
t +30	19.0	2nd stage ignition
t +56	65.5	2nd stage burnout
t +68	90.0	Nosecone separation
t +70	95.0	Start of ACS pointing maneuver
t +297	327.0	Apogee
t +528	90.0	Start of SHEFEX experiment phase
t +560	20.0	End of SHEFEX experiment phase
T +561	18.0	2nd stage separation
T +570	6.8	Start of recovery sequence

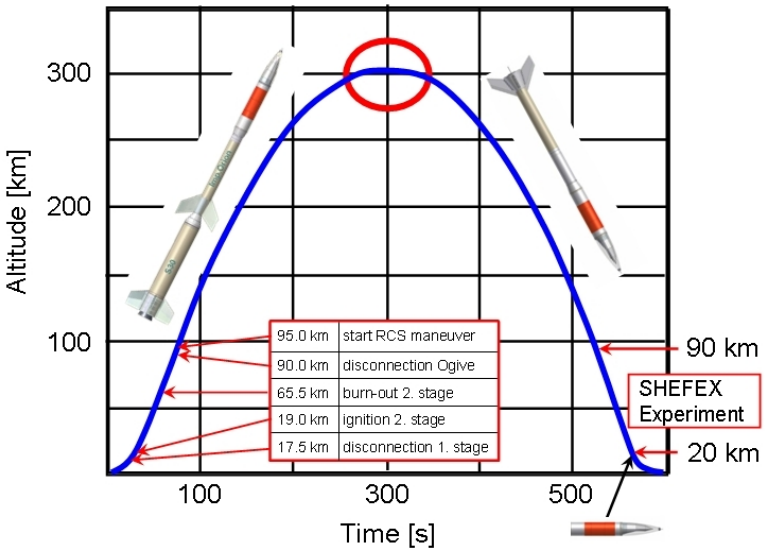

Fig. 4: Projected SHEFEX mission

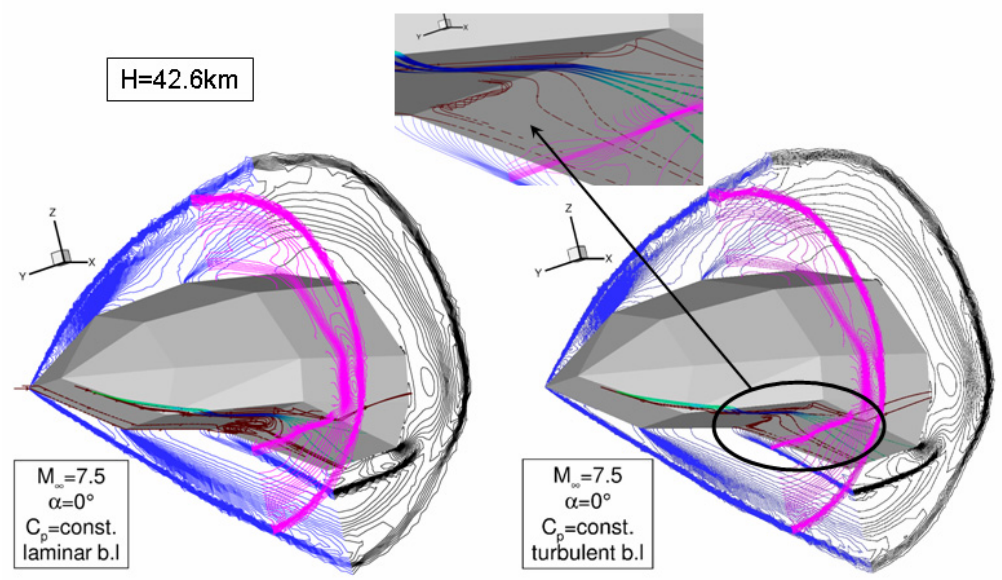

Fig. 5: Influence of the boundary layer state on the flow field, H=42km

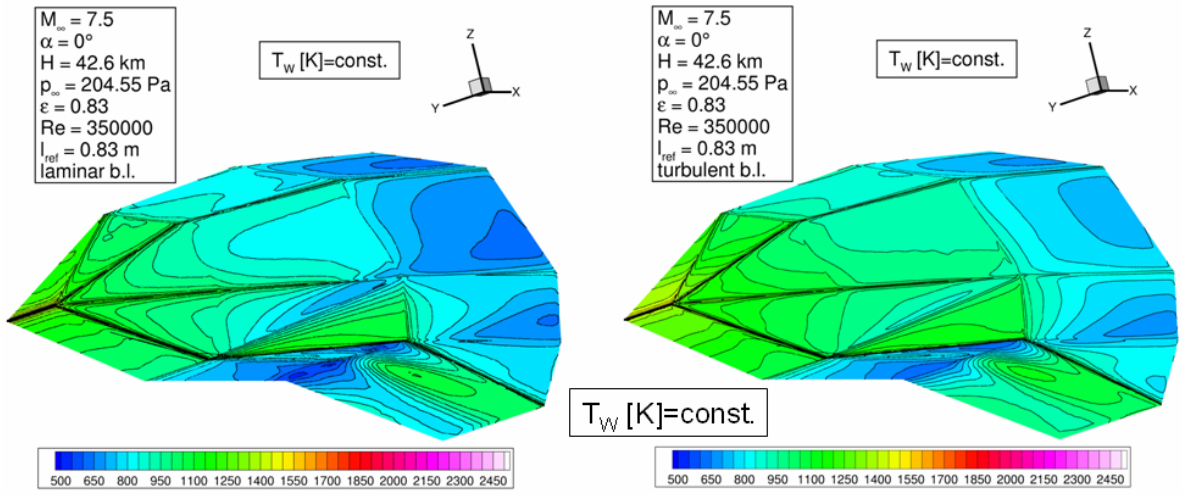

Fig. 6: Influence of the boundary layer state on the surface temperature, H=42km

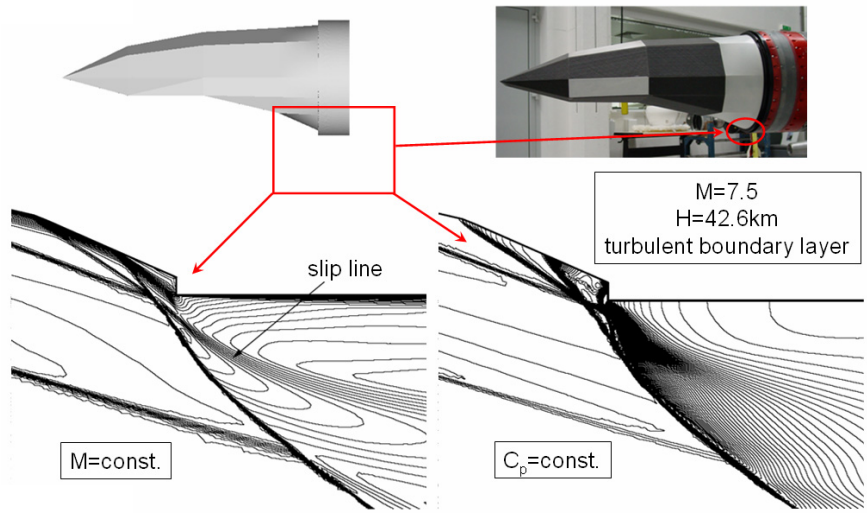

Fig. 7: Flow topology in the symmetry plane

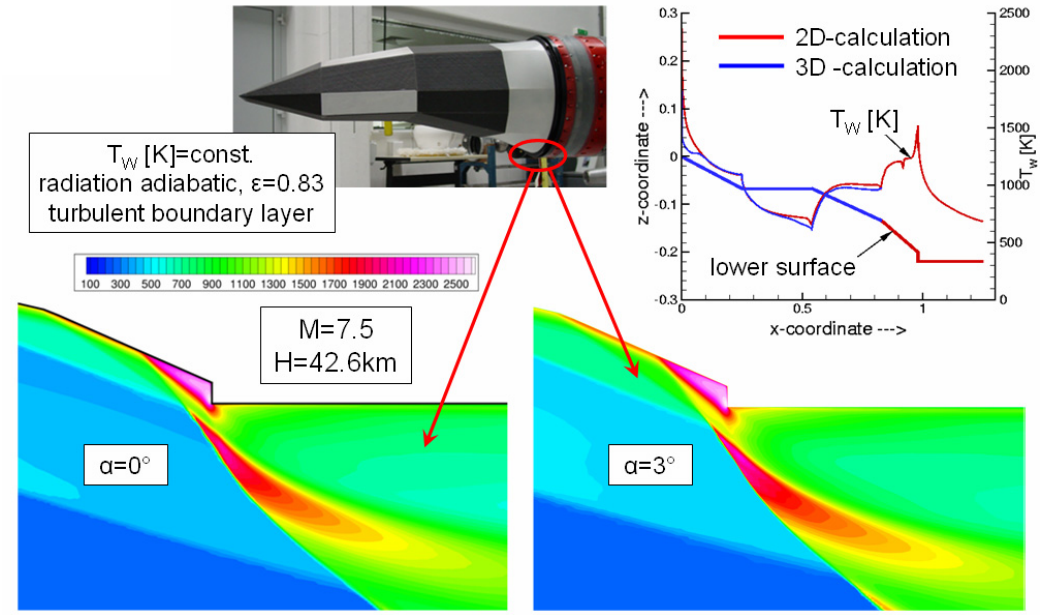

Fig. 8: Influence of angle of attack on the temperature

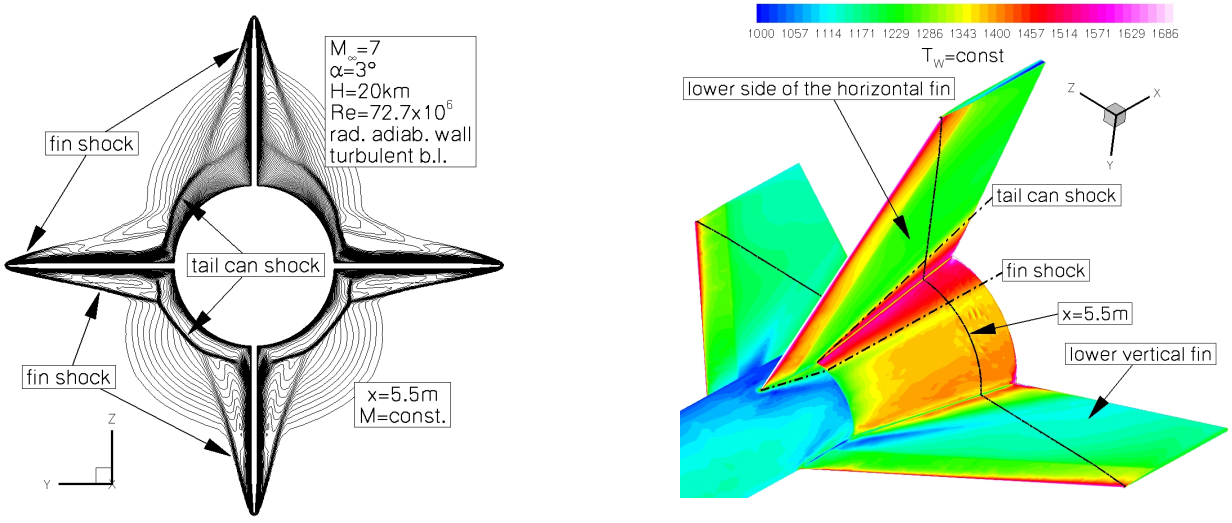

Fig. 9: Analysis of the flow field in the aft region of the reentry configuration

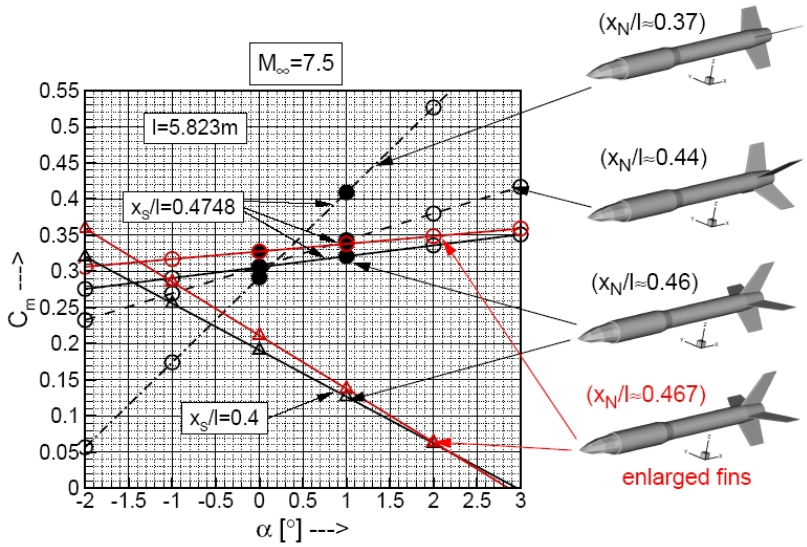

Fig. 10: Reentry pitch stability for various fin arrangements

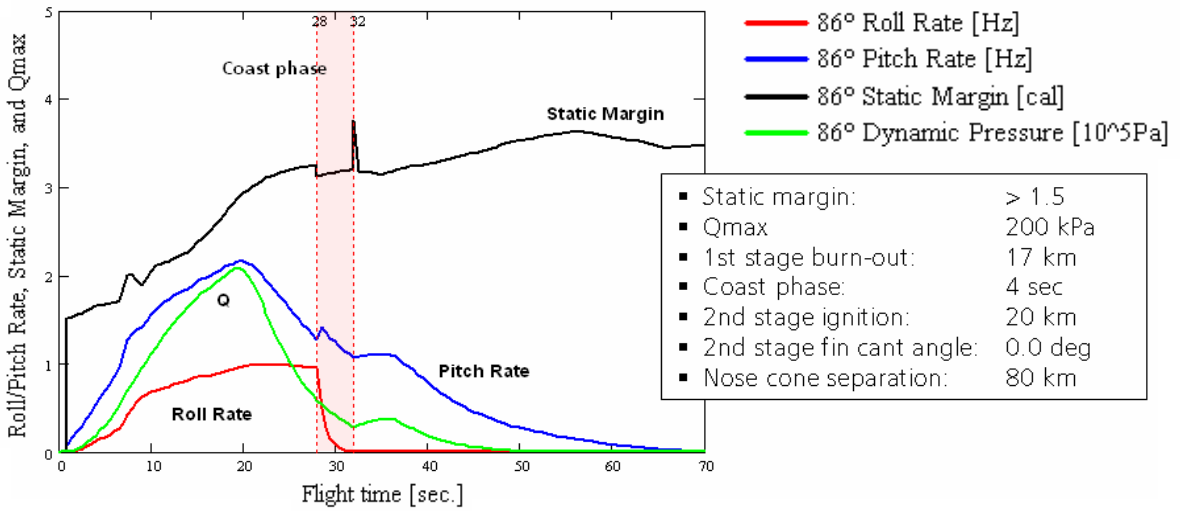

Fig. 11: Ascent pitch and roll rates and static margin

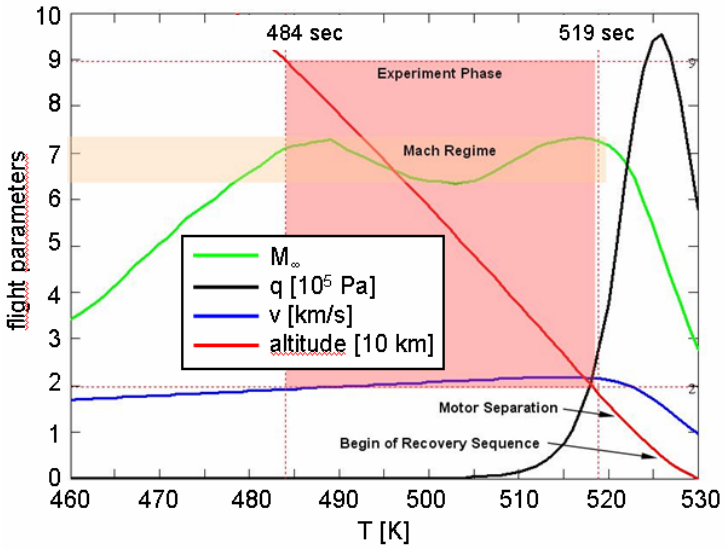

Fig. 12: Predicted re-entry parameters

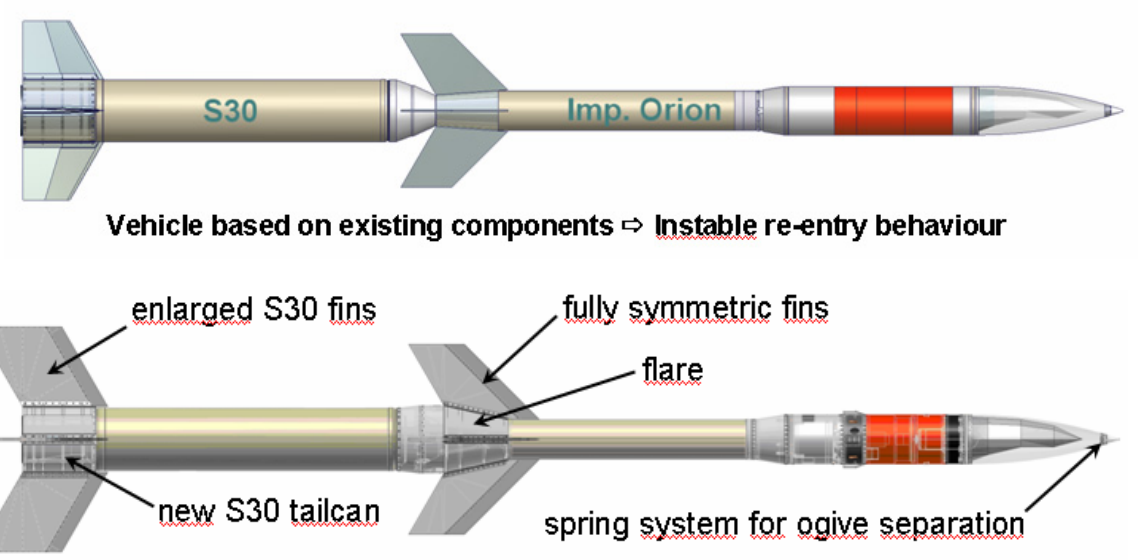

Fig. 13: Standard and final vehicle

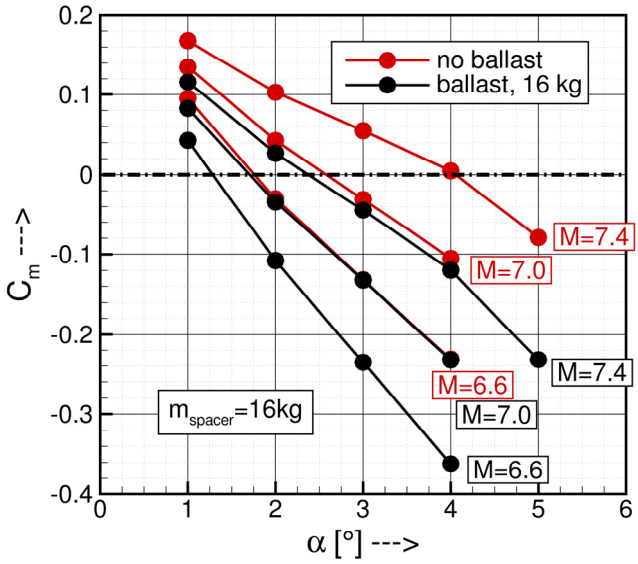

Fig. 14: Pitching moment coefficients of the final reentry vehicle

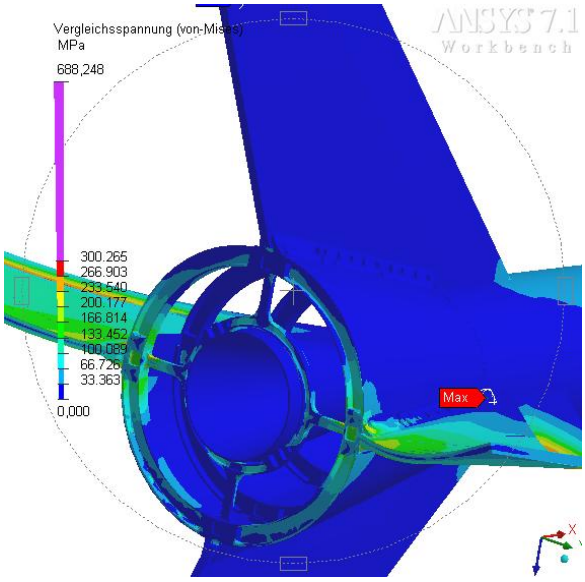

Fig. 15: 2nd Stage Tailcan and Fins (FEM Analysis, Stress Distribution)

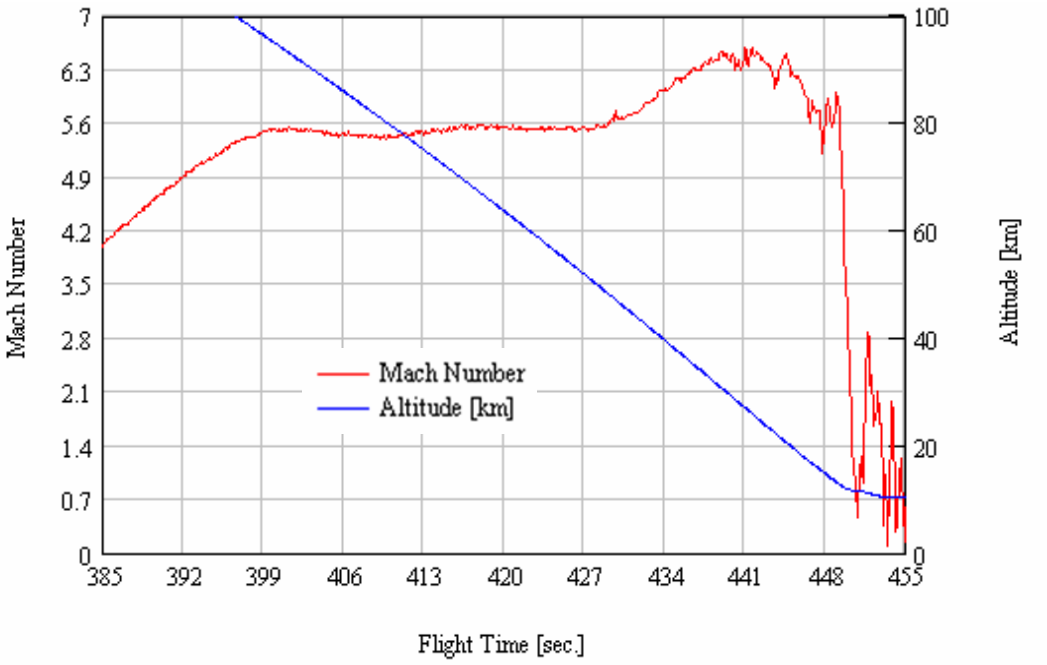

Fig. 16: Altitude over Earth Curvature (Radar Data)

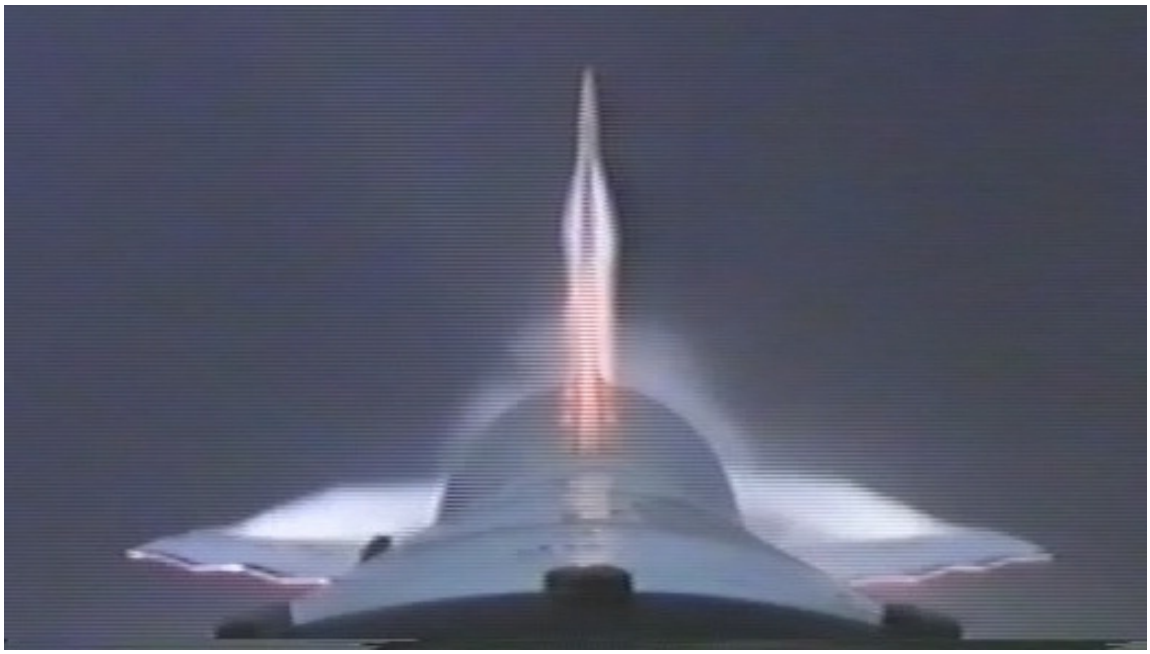

Fig. 17: Vehicle during Re-entry at approximately 18 km on the Down-leg (On-Board Camera)